# Multiple Tissue Pharmacodynamic Analysis of TCDD-Induced Biochemical Responses

Michael J. Santostefano*, Xiaofeng Wang*, Michael J. Devito†,
Vicki M. Richardson†, David G. Ross† and Linda S. Birnbaum†
*Curriculum in Toxicology, Univ. of North Carolina at Chapel Hill, Chapel Hill, NC 27599 USA
†US Environmental Protection Agency, NHEERL, ETD, RTP, NC 27711 USA

**Abstract**

The induction of CYP1A2 by 2,3,7,8-tetrachlorodibenzo-*p*-dioxin (TCDD) and the demonstration that CYP1A2 is responsible for hepatic TCDD sequestration suggest that both pharmacokinetic and pharmacodynamic events must be incorporated for a quantitative description of TCDD disposition. In this paper, a biologically-based pharmacodynamic (BBPD) model was developed to describe the time-dependent increase in TCDD-induced cytochrome P-450 protein expression and associated enzymatic activities in multiple target tissues (liver, lungs, kidneys and skin) by incorporating a time-delay in CYP1A1/1A2 protein expression. This BBPD model illustrates that a similar mechanism for the time-dependent increase in TCDD-induced CYP1A1 protein expression and associated EROD activity exists in multiple target tissues. In addition, this BBPD model quantitatively describes the time-dependent effects of TCDD on induced CYP1A1/1A2 protein expression and associated enzyme activities in multiple target tissues for the first time and provides further confirmation of the potential use of PBPK/BBPD models in exposure analysis and risk assessment.

**Introduction**

Physiologically-based pharmacokinetic (PBPK) and biologically-based pharmacodynamic (BBPD) models serve as state-of-the-art prototypes for interspecies extrapolations employed in risk assessment[1]. Previous pharmacodynamic models for TCDD have focused on TCDD-induced responses in liver[1-9]. In this paper, a BBPD model was developed to analyze the effects of TCDD on cytochrome P-450 protein expression and associated enzyme activity in multiple target tissues (liver, lungs, skin and kidneys) for TCDD-mediated toxicity and biochemical responses[10] in female Sprague-Dawley rats dosed orally with 10 μg TCDD/kg after 30 min, 1, 3, 8 or 24 hours or 7, 14 or 35 days.

**Experimental Methods**

Chemicals 2,3,7,8-Tetrachloro[1,6-$^3$H]dibenzo-*p*-dioxin and unlabeled TCDD were obtained from commercial sources as described[11].

Treatment and tissue isolation Eight week-old female Sprague-Dawley rats were administered a single oral dose of either a corn oil solution containing 10 μg [$^3$H]TCDD/kg body weight (bw) or corn oil vehicle alone at 5 ml/kg bw[11]. At 30 min, 1, 3, 8 or 24 hr or 7, 14 or 35 days after dosing, rats were euthanized by $CO_2$ asphyxiation. The liver, lungs, skin and kidneys were excised and stored at -80°C until usage. All data are represented as the mean ± standard deviation.

CYP1A1/CYP1A2 protein and enzymatic assays The CYP1A1/CYP1A2 protein concentrations and ethoxyresorufin *O*-deethylase (EROD)/methoxyresorufin *O*-demethylase (MROD) activities, were quantitated as described previously[11].

Model development The PBPK model structure and associated mathematical expressions for TCDD in the female Sprague-Dawley rat were reported previously[9]. In this paper, the BBPD model structure for TCDD-induced cytochrome P-450 protein expression and associated enyzmatic activities in multiple target tissues was developed and linked to the existing PBPK model[9]. Model simulations were conducted using the SimuSolv® computer program (Dow Chemical Company, Midland, MI, Version 3.0).

## Results

Time-dependent expression of CYP1A1/CYP1A2 proteins and associated enzymes n the liver.

Figures 1 and 2 illustrate the time-dependent increase in TCDD-induced CYP1A1 and CYP1A2 protein expression in the liver of female Sprague-Dawley rats treated with 10 μg TCDD/kg[12]. Based on the above data (Figures 1 & 2), a BBPD model was developed to analyze the time-dependent effects of TCDD on CYP1A1 and CYP1A2 protein expression in the liver. The estimated parameter values are given in Table 1. These parameters accurately simulated the time-dependent effects of TCDD on CYP1A1 protein expression in the liver using the BBPD model within the experimental error (Figure 1). The shape of Figure 2 illustrates that the parameters in Table 1 described the time-dependent increase in CYP1A2 protein expression in the liver up to 35 days post exposure.

Figures 3 shows the time-dependent effects of TCDD on EROD activity in the liver of female Sprague-Dawley rats exposed to 10 μg TCDD/kg. A time-dependent increase in TCDD-induced EROD activity was observed (Figure 3). Seven days (168 hours) post TCDD-treatment, maximal TCDD-induced EROD activity was found in the liver. Figure 3 also demonstrates that the BBPD model accurately described the time-dependent increase in EROD activity in the liver post exposure to TCDD within the experimental error. Figure 4 shows the time-dependent effects of TCDD on MROD activity in the liver of female Sprague-Dawley rats exposed to 10 μg TCDD/kg. A time-dependent increase in TCDD-induced MROD activity was observed (Figure 4). Fourteen days (336 hours) post TCDD-treatment, maximal TCDD-induced MROD activity was found, which remained elevated at 840 hours (35 days) after TCDD exposure. The shape of Figure 4 illustrates that the parameters in Table 1 described the time-dependent increase in MROD activity in the liver up to 35 days post exposure within the experimental error. The BBPD model slightly under predicted the time for maximal MROD activity in the liver of female Sprague-Dawley rats. For example, the BBPD model simulated a maximal MROD activity appromately 7 days after exposure to a single oral dose of TCDD. However, the experimental data suggests that maximal TCDD-induced MROD activity was obtained 14 days after exposure to a single oral dose of TCDD.

Time-dependent expression of CYP1A1 protein and EROD activity in extrahepatic tissues.

Figure 3 shows the time-dependent effects of TCDD on EROD activity in the lungs, kidneys, and skin of female Sprague-Dawley rats exposed to 10 μg TCDD/kg. In all tissues examined, a time-dependent increase in TCDD-induced EROD activity was observed (Figure 3). Seven days (168 hours) post TCDD-treatment, maximal TCDD-induced EROD activity was found in all tissues. Based on the above data (Figure 3), the BBPD model was also used to simulate the time-dependent increase in EROD activity in extrahepatic tissues. Figure 3 demonstrates that the BBPD model accurately described the time-dependent increase in EROD activity in the lungs, kidneys and skin post exposure to TCDD. The linear coefficient (Table 1) between EROD and CYP1A1 obtained from the liver was then employed to estimate the CYP1A1 concentration in the extrahepatic tissues. The results are shown in Figure 1. The BBPD model predicts that TCDD causes a similar time-dependent increase in CYP1A1 protein expression in the lungs, kidneys and skin as in the liver (Figure 1).

## Discussion

The ability of TCDD to induce CYP1A2, the putative TCDD-binding protein, appears to be the mechanism for maintenance of high concentrations of TCDD in the liver, suggesting that both pharmacokinetic and pharmacodynamic events must be incorporated for a quantitative description of TCDD disposition. Since the induction of CYP1A2 influences the tissue disposition of TCDD,

a BBPD model combined with a PBPK model[9] is necessary for a quantitative description of both TCDD tissue disposition and TCDD-induced biochemical responses. The BBPD model was developed based on the AhR-mediated cytochrome P-450 protein expression and associated enzyme induction in the liver by TCDD. Due to the time-dependent process of TCDD:AhR complex formation and subsequent gene activation, this BBPD model incorporated a time delay in protein expression. This BBPD model differs from the previous PBPK/BBPD response model[8], since it describes the time-course effects of TCDD on CYP1A1/CYP1A2 protein expression and associated enzymatic activities in multiple tissues (Figures 1-4). The parameter values obtained from the present study (Table 1) accurately described the time-dependent effects of TCDD on CYP1A1/CYP1A2 dependent enzymatic activities (or CYP1A1/CYP1A2 protein concentration) (Figures 1-4) without any change in the PBPK model[9] for the time-dependent tissue disposition of TCDD (data not shown).

**Summary.**

This BBPD model quantitatively describes the time-dependent effects of TCDD on induced CYP1A1/CYP1A2 protein expression and associated enzyme activities for the first time in multiple target tissues and provides further confirmation of the potential use of PBPK/BBPD models in exposure analysis and risk assessment.

**Acknowledgements.**

The project described was supported by grant number 1 F32 ES05701-01A1 from the National Institute of Environmental Health Sciences (NIEHS), NIH. Its contents are solely the responsibility of the authors and do not necessarily represent the official views of the NIEHS, NIH. Additional financial support for this research was provided by the US Environmental Protection Agency Cooperative Training Agreement (#T-901915-02) with the University of North Carolina, Chapel Hill, NC 27599-7270. This abstract does not represent USEPA policy. The material has been approved for publication through internal Agency review. The mention of trade names and commercial products does not constitute endorsement or use recommendation.

**Literature Cited**

1. Buckley, L.A., (1995). *Toxicol.* **102**. 125-131.
2. Andersen, M.E., J.J. Mills, M.L. Gargas, L. Kedderis, L.S. Birnbaum, D. Neubert, and W.F. Greenlee, (1993). *Risk Anal.* **13**. 25-36.
3. Buckley-Kedderis, L.B., J.J. Mills, M.E. Andersen, and L.S. Birnbaum, (1993). *Toxicol. Appl. Pharmacol.* **121**. 87-98.
4. Kohn, M.C., G.W. Lucier, G.C. Clark, C. Sewall, A.M. Tritscher, and C.J. Portier, (1993). *Toxicol. Appl. Pharmacol.* **120**. 138-154.
5. Kohn, M.C., C.H. Sewall, G.W. Lucier, and C.J. Portier, (1996). *Toxicol. Appl. Pharmacol.* **165**. 29-48.
6. Leung, H.W., R.H. Ku, D.J. Paustenbach, and M.E. Andersen, (1988). *Toxicol. Lett.* **42**. 15-28.
7. Leung, H.W., D.J. Paustenbach, F.J. Murray, and M.E. Andersen, (1990). *Toxicol. Appl. Pharmacol.* **103**. 399-410.
8. Roth, W.L., S. Ernst, L.W.D. Weber, L. Kerecsen, and K.K. Rozman, (1994). *Toxicol. Appl. Pharmacol.* **127**. 151-162.
9. Wang, X., M.J. Santostefano, M.V. Evans, V.M. Richardson, J.J. Diliberto, and L.S. Birnbaum, (1997). *Toxicol. Appl. Pharmacol.* (Submitted).
10. Birnbaum, L.S., (1994). *Environ. Hlth. Perspec.* **102**. 157-167.
11. Santostefano, M.J., K.L. Johnson, N.A. Whisnant, V.M. Richardson, M.J. DeVito, J.J. Diliberto, and L.S. Birnbaum, (1996). *Fundam. Appl. Toxicol.* **34**. 265-275.
12. Santostefano, M.J., D.G. Ross, U. Savas, C.R. Jefocate, and L.S. Birnbaum, (1997). *Biochem. Biophys.Res. Comm.* **233**. 20-24.

Table 1. Results of Parameter Estimation

| Model parameters | Values | Parameter estimation |
|---|---|---|
| Liver Weight (g) | 9.05 | measured |
| Lungs Weight (g) | 0.81 | measured |
| Skin Weight (g) | 45.80 | measured |
| Kidneys Weight (g) | 1.64 | measured |
| **CYP1A2**[a] | | |
| Basal Concentration (nmole/g) | 1.6 | reference 9 |
| Degradation rate ($hr^{-1}$) | 0.1 | reference 9 |
| Maximum induction fold for CYP1A2 | 600.0 | reference 9 |
| TCDD:Ah:DNA to induce CYP1A2 (nM) | 130.0 | reference 9 |
| TCDD:CYP1A2 (nM) | 35. | reference 9 |
| Hill coefficient | 0.6 | reference 9 |
| # compartments to simulate delay | 3 | Estimated from BBPD |
| Holding time for delay (hr) | 2 | Estimated from BBPD |
| **CYP1A1**[a] | | |
| TCDD:Ah:DNA (CYP1A1) (nM) | 10 | reference 9 |
| Hill coefficient (nM) | 1 | reference 9 |
| Linear coefficient between EROD & CYP1A1 (EROD activity/CYP1A1 protein) | 1500 | Estimated from BBPD model |
| # compartments to simulate delay | 3 | Estimated from BBPD |
| Holding time for delay (hr) | 2 (Li)<br>1 (Lg)<br>1 (K)<br>0.2 (S) | Estimated from BBPD |
| **EROD activity**[b] | | |
| Basal EROD activity (liver) | 270.6 | Constitutive EROD activity |
| Basal EROD activity (lungs) | 6.72 | Constitutive EROD activity |
| Basal EROD activity (kidneys) | 141.1 | Constitutive EROD activity |
| Basal EROD activity (skin) | 0.2 | Constitutive EROD activity |
| Degradation rate ($hr^{-1}$) | 0.04 | Estimated from BBPD model |
| Maximum EROD induction rate (activity/hr) in the liver | 900 | Estimated from BBPD model |
| Maximum EROD induction rate (activity/hr) in the lungs | 500 | Estimated from BBPD model |
| Maximum EROD induction rate (activity/hr) in the kidneys | 8000 | Estimated from BBPD model |
| Maximum EROD induction rate (activity/hr) in the skin | 22000 | Estimated from BBPD model |
| **MROD**[b] | | |
| Basal activity (liver) | 58.6 | Constitutive MROD activity |
| Synthesis rate (activity/hr) | 0.01 | Estimated from BBPD model |
| Degradation rate ($hr^{-1}$) | 0.004 | Estimated from BBPD model |
| **AhR** | | |
| TCDD:AhR (nM) | 0.1 | reference 9 |

[a]Optical density/μg microsomal protein. [b]pmoles/min/mg microsomal protein.

**Figure 1**

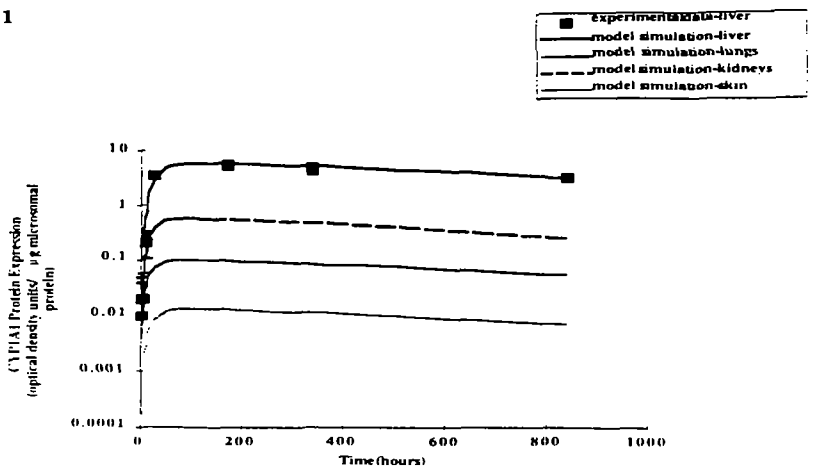


Figure 1. Time-dependent effects of TCDD on CYP1A1 protein expression in the liver, lungs, kidneys and skin of female Sprague-Dawley rats treated with 10 µg TCDD/kg with BBPD model simulation. All symbols were obtained from TCDD-treated animals as described in Materials and Methods section. Solid and broken lines were derived from the BBPD model simulation of the experimental data. Closed squares=hepatic CYP1A1 protein concentration. Data are presented as mean ± standard deviation (n=4-5).

**Figure 2**

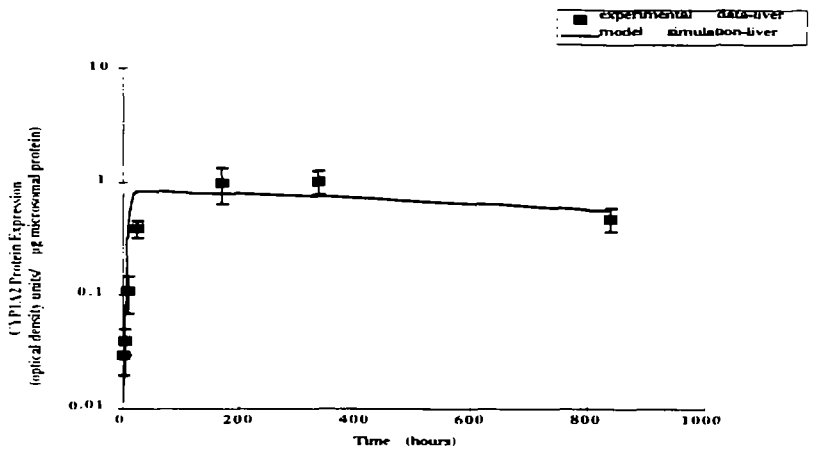


Figure 2 Time-dependent effects of TCDD on CYP1A2 protein expression in the liver of female Sprague-Dawley rats treated with 10 µg TCDD/kg with BBPD model simulation. All symbols were obtained from TCDD-treated animals as described in Materials and Methods section. The solid line was derived from the BBPD model simulation of the experimental data. Closed squares=hepatic CYP1A2 protein concentration. Data are presented as mean ± standard deviation (n=4-5).

**Figure 3**

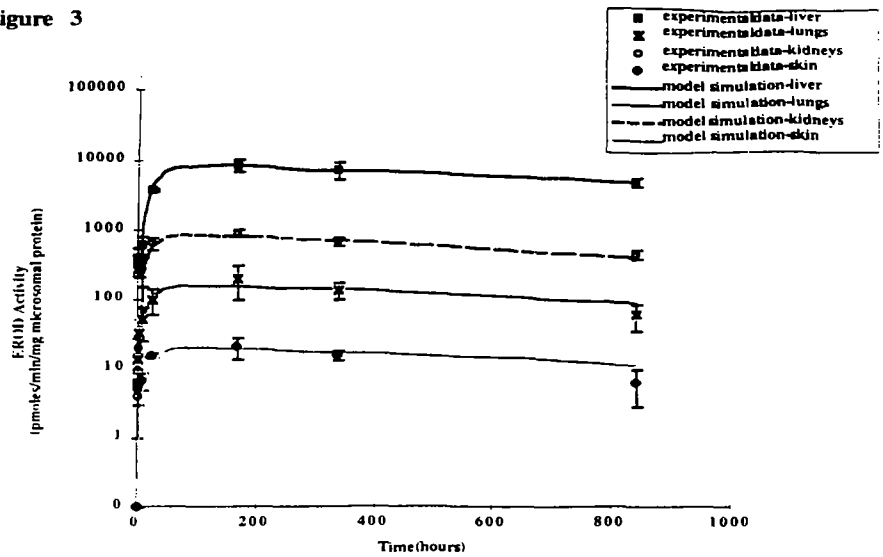


Figure 3. Time-dependent effects of TCDD on EROD activity in the liver, lungs, kidneys and skin of female Sprague-Dawley rats treated with 10 µg TCDD/kg with BBPD model simulation. EROD activity determined from 0-35 days (A). EROD activity determined from 0-24 hours (B). All symbols were obtained from TCDD-treated animals as described in Materials and Methods section. Solid and broken lines were derived from the BBPD model simulation of the experimental data. Closed squares=EROD activity in liver; open circles=EROD activity in kidneys; x=EROD activity in lungs and open diamonds=EROD activity in skin. Data are presented as mean ± standard deviation (n=4-5).

**Figure 4**

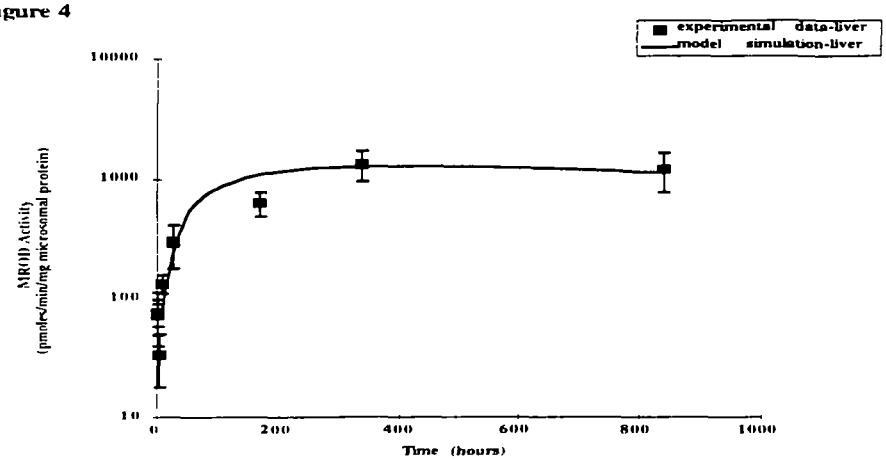


*Figure 4. Time-dependent effects of TCDD on MROD activity in the liver of female* Sprague-Dawley rats treated with 10 µg TCDD/kg with BBPD model simulation. All symbols were obtained from TCDD-treated animals as described in Materials and Methods section. The solid line was derived from the BBPD model simulation of the experimental data. Closed squares=MROD activity in liver. Data are presented as mean ± standard deviation (n=4-5).